Fatigue Life Study for a Railroad Bascule Bridge

CHARLES T. JAHREN AND JOHN A. ROOKER

A fatigue study was undertaken for an 80-year-old drawbridge whose members receive cyclic loading from both draw-span movements and trains. Although the study was a modest effort, a significant amount of information was obtained. Fatigue loading was evaluated by drawing a traffic sample from the railroad's data base and modifying the results in accordance with historical records. Critical bridge members were identified using a three-dimensional linear elastic analysis, and their cyclic stresses were corroborated by the results of experimental work. Then the remaining fatigue life of these members was estimated. The results show that many of the members have a remaining fatigue life of substantial length.

The fatigue life of bridges is a point of concern for the safe and efficient operation of railroads. At a time when wheel loads and traffic are increasing, many important railroad bridges have reached an age of 60 to 100 years. Unnecessary or premature replacement of a bridge is undesirable because the cost is high and funding is scarce. However, because of potential safety problems and the possibility of disrupted service, fatigue life should not be overestimated. When replacement is necessary, an early prediction for the end of the service life should be provided so that sufficient lead time is available for financial planning and budgeting.

This paper describes a fatigue study for an 80-year-old drawbridge whose members receive cyclic loading from both draw-span movements and trains. Although it was a modest effort, the study included both analytical and experimental work. The results indicate that many of the structural members have a remaining fatigue life of substantial length. This illustrates that significant information can be obtained from a modest research effort.

BACKGROUND

The subject of this study is Burlington Northern's (BN) Bridge 4, a 200-ft-long, double-track bascule bridge located in Seattle, Washington. The design was by the Strauss Trunnion Bridge Company. The node numbering system for the analysis and other dimensions are given in Figure 1. When the bridge draws, the moving leaf tilts up on the main trunnion. A counterweight is connected to the moving leaf through a series of links and hinges such that the top chord is in tension and the bottom chord is in compression unless a train is on the bridge. The bridge was built in 1913 of riveted steel with built-up members and has a Cooper's rating of E55 based on an allowable stress of 16 ksi. Present American Association of Railway Engineers (AREA) (*1*) design criteria call for bridges to be designed to a Cooper's rating of E80.

Primarily used by time-sensitive intermodal trains, the bridge is at a critical location in BN's Pacific Northwest railroad network. A closure would be very disruptive because trains would have to make time-consuming detours. Because of age, load rating, critical location, and expected increases in high-axle-load intermodal traffic, it was desirable to know the potential for fatigue cracking and the members that are most likely to be affected. The study focused on the bridge's moving leaf; neither the machinery nor the counterweight truss and tower were investigated.

To estimate fatigue life, it is necessary to have information on the loads, the resulting cyclic stresses, and the fatigue resistance. In past studies on other bridges, estimates for loads have been developed from traffic surveys and historical records (*2–4*); estimates of cyclic stresses were obtained from structural analysis (*2,5*) and field instrumentation (*3,4,6,7*); and fatigue resistance was based on AREA or AASHTO S-N relationships. Current research is providing additional information on railroad load spectrums and bridge fatigue behavior (*8*).

The fatigue loads for this study were based on a sample of 72 trains drawn from traffic that crossed the bridge during the 6-month period starting in March 1989. The sample consisted primarily of intermodal and general freight trains with a few coal or grain trains (Table 1). Later in the study, adjustments were made in the cyclic stresses to account for historical changes in wheel loads. These adjustments will be described later.

A three dimensional linear-elastic structural analysis provided cyclic stress information that was corroborated by the results of a limited field instrumentation effort. Based on the results of the structural analysis, critical members were selected for further analysis, and the AREA and AASHTO S-N relationships were used to provide estimates of fatigue resistance.

LOAD EVALUATION

As part of normal record-keeping activities, before a train departs, a list of cars is drawn up and entered into a computer data base. For each rail car, the list gives the serial number, gross weight, contents, destination, and a code that denotes the type of car (Figure 2). BN's car type code has four characters and is referred to as a GST code. The identification

C. T. Jahren, Department of Civil Engineering, University of Washington, 121 More Hall FX-10, Seattle, Wash. 98195. J. A. Rooker, Geiger Engineers, 110 Prospect Street, Bellingham, Wash. 98225.

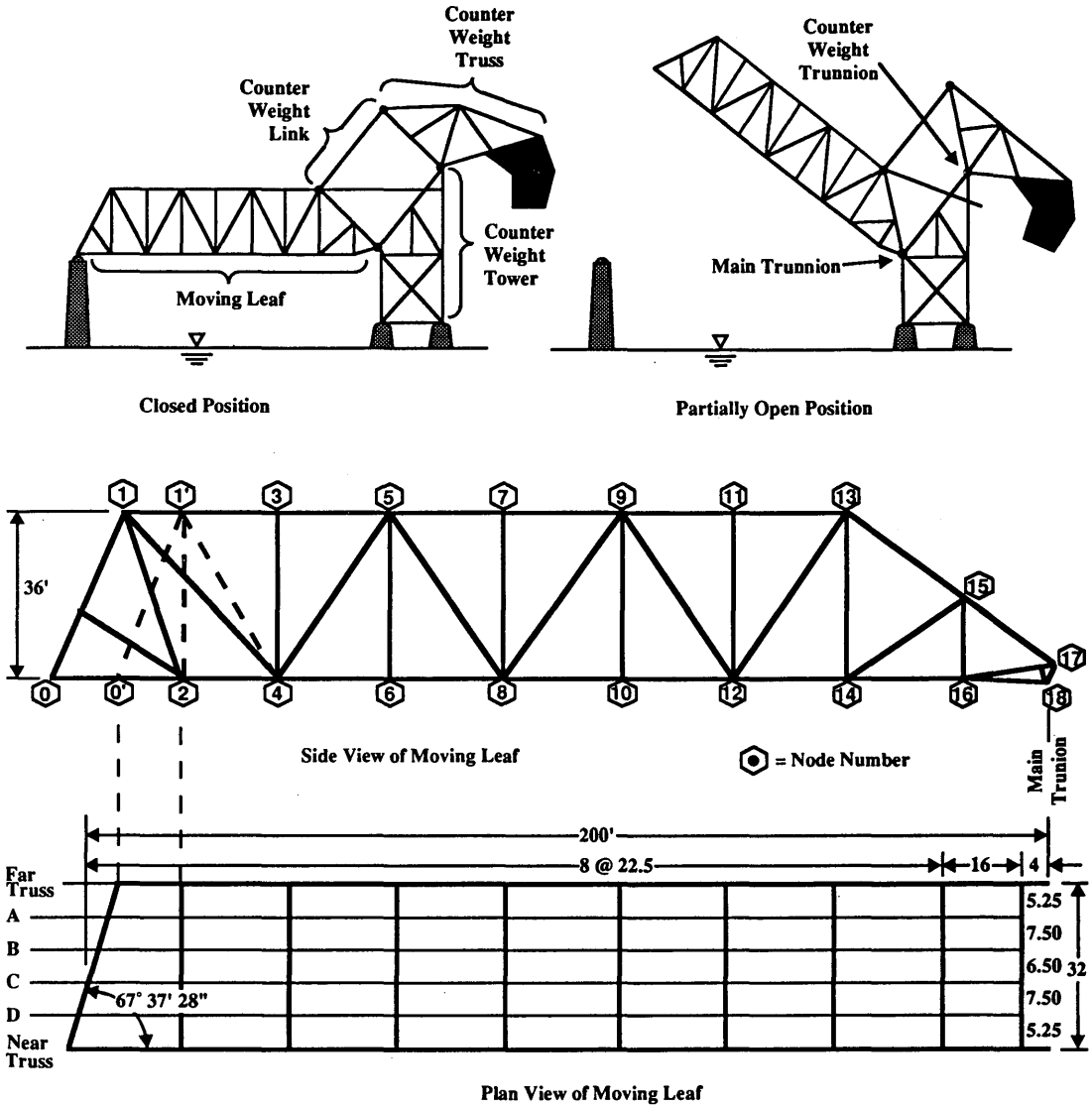

FIGURE 1 BN Bridge No. 4 (drawings not to scale).

TABLE 1 Sample of 72 Trains, 1988–1989

Train Type	No. of Trains	Percent	Trailing Tonnage	Percent
Intermodal (all types)				
Empty	11	15	22,346	14
Single stack	15	21	35,766	22
Double stack	4	6	9,571	6
Total	30	42	67,683	42
General freight	27	38	68,125	42
Grain/coal	9	12	26,016	16
Locomotives[a]	6	8	79	0
Total	72	100	161,903	100
Average train			2,249	

[a]Locomotives running light without a train.

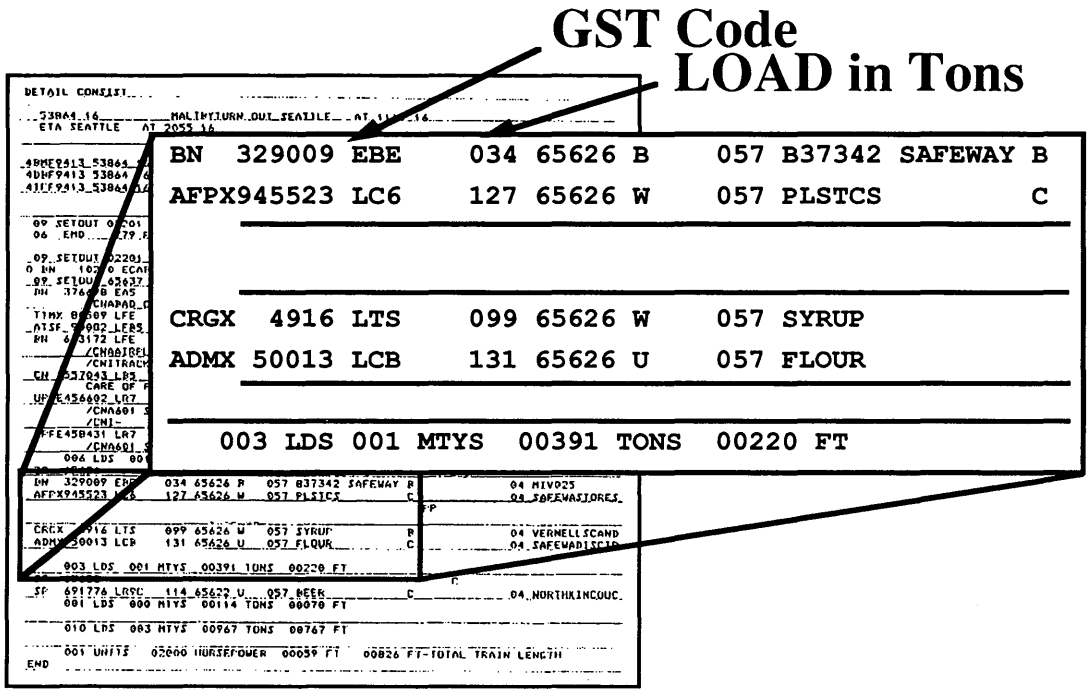

FIGURE 2 Train list from data base.

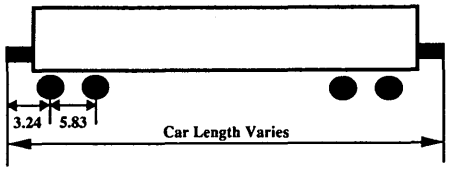

(a) Freight Car (Wheel Load Varies)

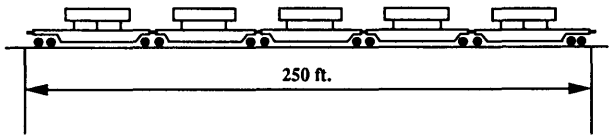

(b) Five Unit Articulated Intermodel Car (Wheel Load Varies)

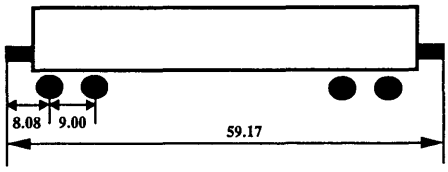

(c) Four Axle Locomotive (Wheel Load = 33 Kips)

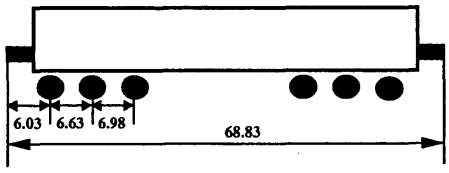

(d) Six Axle Locomotive (Wheel Load = 33 Kips)

FIGURE 3 Rail car and locomotive geometry.

number and length of each locomotive are also given. A FORTRAN program was developed that reads the gross weight and GST code for each car and generates a load string that gives estimated axle loads and spacings.

The axle loads were estimated by dividing the gross weight of the car equally among its axles. An exception was the five-platform articulated intermodal car having load platforms that share axles (Figure 3*b*). For these cars, the gross weight refers to the combined gross weight of all platforms. Each axle in an articulated wheel set was assigned one-tenth of the gross weight of the car, whereas each axle in an end wheel set was assigned one-twentieth of the gross weight.

It is possible to estimate the axle spacing from the GST code, because the length of the car may be inferred from the GST code to an accuracy of ± 5 ft and because the location of the axles in relation to the end of a rail car is consistent (Figure 3*a*). The program read the GST code, consulted a list that provided axle geometries for each car code, and computed the axle spacing.

Although there are many types of locomotives with various load characteristics, this program modeled two basic types of locomotives. Locomotives $\leq$ 62 ft long were assigned four axles (Figure 3*c*), and locomotives $>$ 62 ft long were assigned six axles (Figure 3*d*). Wheel loads were from 31 to 34 kips, depending on the length of the locomotive.

Because the resulting load string is based on several estimates, it is appropriate to discuss whether its quality is sufficient for use in fatigue studies. The gross car weight is entered by a clerk who scans a shipping document to find the weight of the contents and then guesses the tare weight of the rail car. Rail cars are rarely weighed before shipping and, for a variety of reasons, the net weight on the document may not be the actual weight of the contents. Furthermore, the contents of the rail car may be unevenly loaded. Despite these

shortcomings a weigh-in-motion comparison for three trains showed that these load models were useful for fatigue studies. Lists were obtained for the three trains and converted to a load string. Using the process described in the next section, the equivalent stress range for the midspan of a typical stringer was calculated for each train. Individual wheel loads were obtained for the same trains from the weigh-in-motion scale. Then the wheel loads from the list were replaced by the wheel loads from the weigh-in-motion scale and the stress range calculation was repeated. The differences ranged from 2 to 7 percent. If a sample contains several such trains, the difference of the whole sample is likely to be much smaller.

ANALYSIS OF STRESS CYCLING

As part of the effort to account for cyclic stresses, a three-dimensional model of the bridge was developed using the SAP 90 (*9*) structural analysis program (*10*). Except as noted later, the bridge was modeled as a rigid frame because the truss joints were heavy gusseted connections. The stringer-to-floor-beam connections had moments released in the major and minor axis because the actual connections were clip angles that joined only the webs of the members. Moments were also released for light cross-bracing members. Supports at the trunnion end (Node 17) were restrained against translation and rotation, except for rotation about the trunnion axis. The effect of the counterweight link was modeled by imposing forces in the appropriate location (Node 13) and direction. For the dead load condition, the support at the open end of far truss (Node 0) had no restraints, and the support for the near truss had only a vertical restraint that was required for structural stability; the force in the latter was negligible. For the live load condition, both the near and far trusses had vertical supports at the open end (Node 0). The dead load was modeled as the gross section of the bridge members, a line load to account for the track components, and a scaling factor to account for connection plates and other components that were not modeled.

The cyclic loading caused by draw span movement was modeled by rotating the moving leaf about the axis of the trunnion, making necessary alterations to the counterweight forces and recording the change in dead load stress for each member. Burlington Northern's records indicate that current draw span usage is 255 lifts per month. Historical records could not be found for past draw span movement, so for this study the number of lifts was increased to 300 per month (274,000 from 1913 to 1989) to cover uncertainty for the number of past lifts. The tensile portions of the member stress ranges in the far truss that exceed 3 ksi for a 60-degree lift are shown in Figure 4*a*. These stress cycles represent the largest stress cycle in the member when both bending moment and axial force are considered. Similar stresses were found in the near truss.

The tensile portions of the member stress ranges in the far truss that exceed 3 ksi for two 6-axle locomotives (Figure 3*d*) are shown in Figure 4*b*. For some members, the locomotive and draw span stress cycles are additive when trains cross the bridge between lifts. For example, end post Member 13-15 (Figure 5*a*) has a dead load stress of 5.0 ksi. Unlike end post

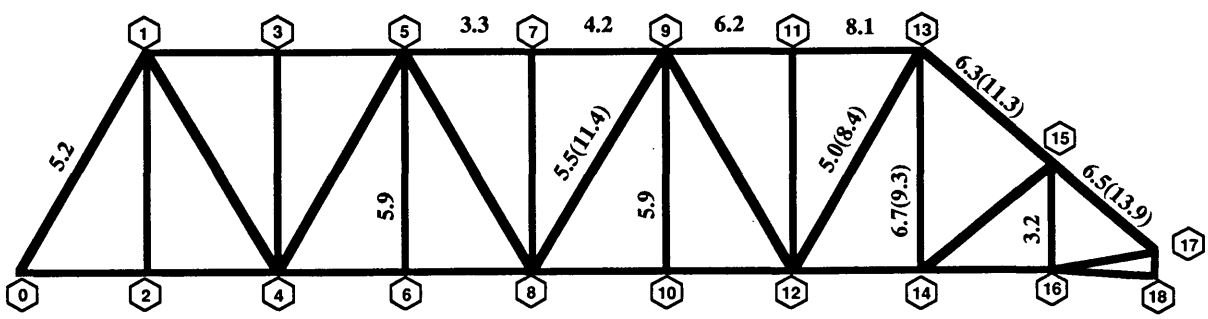

(a) Draw Span Motion, Lift Angle = 60°

Number in parentheses denotes stress range for sequential draw span motion and locomotive movement.

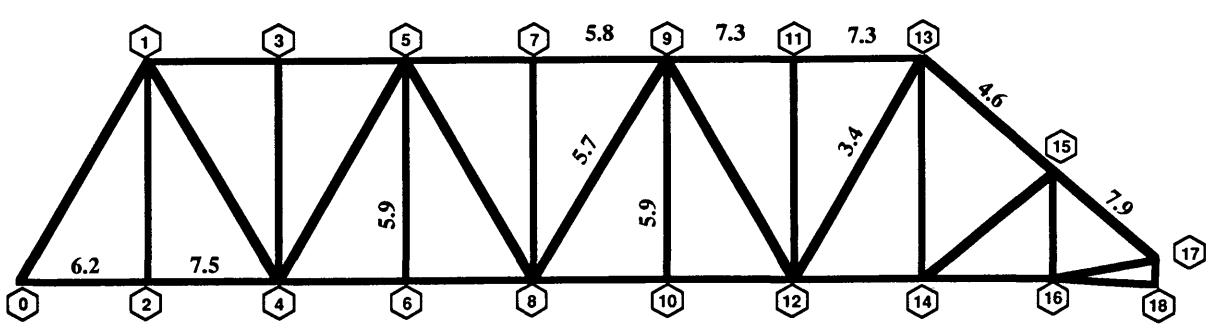

(b) Locomotive Movement

● = Node Number

FIGURE 4 Cyclic stresses greater than 3 ksi (tensile portions only), far truss.

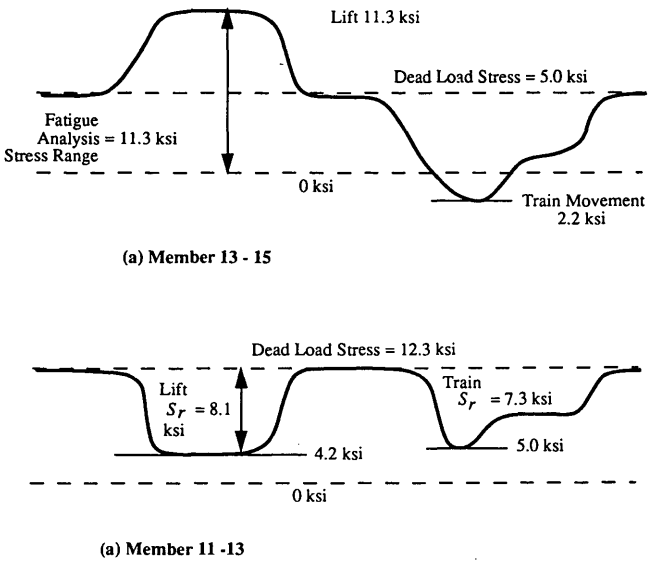

FIGURE 5 Sequential draw span movement.

stresses in most truss bridges, this is a tensile stress, because of the influence of the counterweight link. During a lift the stress increases to 11.3 ksi and, during train movement, the member receives a 2.2-ksi compressive stress. Thus the tensile portion of the stress cycle that is used for fatigue analysis is 11.3 ksi. Top chord member 11-13 does not receive such additive stress cycles (Figure 5*b*). The dead load stress is 12.3 ksi. Lifting the bridge reduces the stress to 4.2 ksi. Similarly, train movement reduces the stress to 5.1 ksi. For fatigue analysis, these cycles may be counted as separate cycles of 8.1 and 7.3 ksi, respectively. In cases in which the stress cycles are additive, the full stress range is shown in parentheses (see Figure 4*a*).

One possible strategy for performing the fatigue analysis was to run the entire sample of 72 load strings on the frame model and then to analyze the cyclic stresses for every member of the bridge. Because the frame model included 228 members, the computational effort rendered that strategy impractical. Instead, a model test load of two 6-axle locomotives (33-kip wheel loads) and four 40-ft cars (19-kip wheel loads) was used (geometry shown in Figure 3), and the resulting cyclic stresses were examined to select six critical members for complete analysis: Top chord 11-13 receives relatively large stress ranges because of both draw span movement and rail traffic. End post 13-15 had a large stress range because of draw span movement. Diagonal 8-9 is a representative diagonal for the bridge. Hangers and stringers are members that receive many cycles and often develop fatigue problems. Therefore, Hanger 13-14, a typical hanger, and a typical stringer were selected (the hangers above Nodes 6 and 10 and the stringers between Nodes 2 and 16 are identical). Because they experienced relatively small stress ranges, the floor beams were not selected.

From the frame model, stress influence lines were developed for each critical member and coded into a FORTRAN program. The load strings were advanced over the influence lines to give a time history of the cyclic stress. These stress histories were converted to stress spectra using a rain flow counting method (*11*); an equivalent constant amplitude stress range, S_{re}, was calculated using a derivation of Miner's rule:

$$S_{re} = (f_i S_{ri}^3)^{1/3} \tag{1}$$

where f_i is the fraction of the stress range within interval i and S_{ri} is the midwidth of the stress interval i. The results of this analysis are shown in Table 2. An example calculation is shown in Figure 6. The tons per cycle (TPC) were calculated by dividing the tonnage of the traffic sample by the number of cycles that each member experienced. Top chord 11-13 and the typical stringer have the largest S_{re}; however, considering TPC, it is apparent that the stringer is subjected to more cyclic loading than the top chord. The stringer receives two cycles (one large and one small) per rail car, whereas the top chord receives about three cycles per train (average gross weight of train = 2,249 tons; see Table 1). BN provided historical information on annual gross tonnage and average gross weight per car from which an estimate of the yearly cyclic stresses was developed. Using Equation 1, a lifetime S_{re} was calculated. The calculations were not altered to reflect changes in car geometry, locomotive geometry, or impact factors. Analysis of stress cycles caused by hypothetical historical trains showed that this simplification has little effect on the final results because draw span motion and modern freight traffic has contributed the most to the bridge's fatigue damage.

Further adjustments were made to the cyclic stresses after reviewing the results of the field instrumentation described in the next section.

TABLE 2 Tons per Cycle and Equivalent Stress Ranges

Member	Tons per Cycle[a]	Current Equivalent Stress Ranges[a] (ksi)	Lifetime Equivalent Stress Range[b] (ksi)
Typical hanger	55.2	3.2	2.9
Framed hanger (13–14)	90.5	2.2	2.0
End post (13–15)	813.6	3.7	3.4
Top chord (11–13)	852.1	4.2	3.8
Diagonal (8–9)	71.2	2.6	2.3
Stringer (Panels 2–16)	46.5	4.3	3.8

[a]Calculated from a sample of 72 trains that crossed Bridge No. 4 in August 1988 (see Table 1).
[b]Adjusted for historical loads.

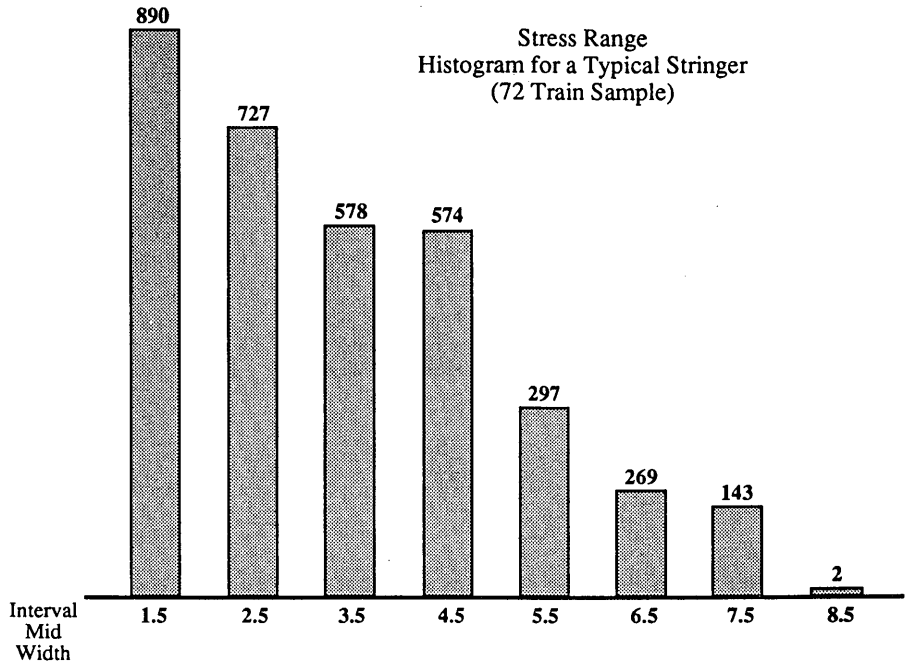

1.5^3	* 890	=	3,004
2.5^3	* 727	=	11,359
3.5^3	* 578	=	24,782
4.5^3	* 574	=	53,306
5.5^3	* 297	=	49,413
6.5^3	* 269	=	73,874
7.5^3	* 143	=	60,328
8.5^3	* 2	=	1,228
Totals	3480		277,294

$$S_{re} = \sqrt[3]{277{,}294 / 3480} = 4.30 \text{ ksi}$$

FIGURE 6 Example of effective stress range calculation.

FIELD INSTRUMENTATION

The experimental portion of this study was performed to confirm the calculated stress ranges for the critical members and to check for stress transients during draw span movement. Strain measurements were taken at a typical stringer (midspan Panel 2-4), a typical hanger (9-10, 81 in. above Node 10), and the top chord near the counterweight link (11-13, 107 in. from Node 13). The instruments were located on the near truss because more heavily loaded trains were expected on the near track. Later observations, however, showed that loaded trains used both tracks equally. The strain gauges were read and digitally recorded by a personal computer equipped with a data acquisition board.

A comparison was drawn between the stresses inferred from the strain-time plots of two SD40-2 locomotives (33-kip wheel load; Figure 3*d*) traversing the bridge at crawl speed and the analytical result for the same load. The stress history for the bottom flange of the stringer is shown in Figure 7*a*. The four peaks in stress correspond to the four locomotive trucks, and the stress reversals indicate that there is some fixity in the stringer-to-floor-beam connection. The stress inferred from the instrumentation for the top flange 8.9 to 10.6 ksi (compressive portion of stress range only) and the bottom flange was between 5.0 and 6.8 ksi (tensile portion of stress range only). The analytical comparison for both the compression and tension flanges was 6.9 ksi. The angles of the top flange of the stringers had been replaced, and the replacement may have caused a redistribution of stresses that would account for the higher compressive stresses found in the top flanges.

The hanger is an H-shaped built-up member consisting of a web plate and four flange angles that serve as flanges. The floor beam is riveted to the inside flange angles of the hanger. For the hanger, the strain readings on the flange exceeded those at the neutral axis by as much as 20 percent and indicated the existence of bending stresses, as shown in Figure 8. Fisher and Daniels (*6*) observed similar bending stresses in hangers of railroad bridges. Shear lag in the stringer-to-floor-beam connection may cause a further increase in stress on the inside flange of the hanger because strain in the outside flange is not mobilized.

The top chord is a box-shaped member. Strain gauges were located on the top of one web plate and the bottom of the other web plate, as shown in the legend of Figure 7*b*. The stress range at the top of the member was larger than at the bottom, indicating that the member experiences some bending. The frame analysis predicted the presence of bending at this location but the stress ranges from instrumentation ex-

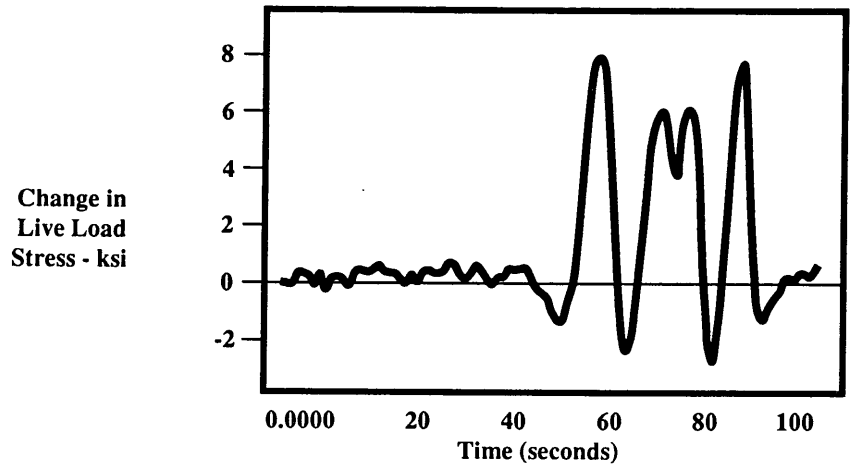

(a) Stringer, Lower Flange, 6 Axle Locomotive

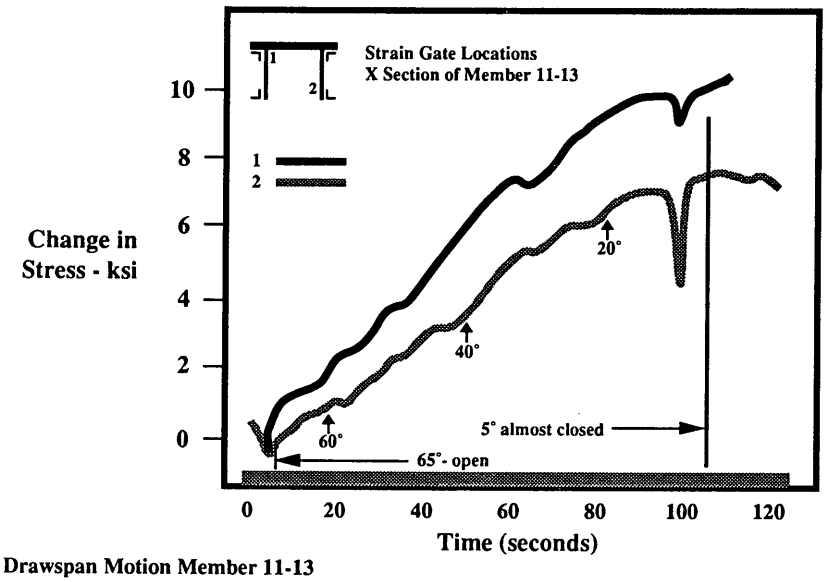

(b) Drawspan Motion Member 11-13

FIGURE 7 Field test results.

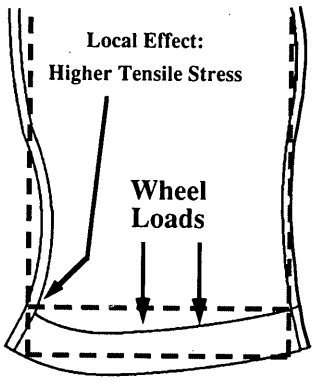

FIGURE 8 Deformed floor beam.

ceeded those from the frame analysis. Time histories of stresses in the top chord members were recorded during the draw span movement. The draw span was brought to a jerking halt several times so that any resulting impact strains could be recorded. The stress history is shown in Figure 7*b*. The measurements indicate that a stress range of 3.8 ksi results from this jerking action.

Results from the frame analysis suggested that the expected vibrational period was 0.5 sec; however, no vibrational stresses of this period were detected by the instrumentation during rail traffic or draw span motion.

The structural model was also checked using optical surveying methods. Using frame analysis, an estimate of the midspan deflection of the truss (0.07 ft) was calculated for the load of two SD 40-2 locomotives. Readings with an engineer's level gave the same result.

FATIGUE EVALUATION

Rivet holes are often the critical details that initiate fatigue cracks in riveted bridges. For built-up members, initial cracking can be expected after the stress exceeds the Category D curve; however, since several components must crack before a built-up section collapses, Category C is an appropriate fatigue life limit (*12*). For all critical members, Table 3 presents estimates of D, the amount of fatigue damage caused by draw span movement or rail traffic (stringers are not affected by drawspan movement). D_i is calculated by

$$D_i = \frac{n_i}{N_i} \tag{2}$$

where n_i is the number of stress cycles in a particular stress range and N_i is the number of cycles allowed by the appropriate S-N relationship. The summation of D_i gives D the total fatigue damage. Fatigue life ends when $D = 1$. Except for a set of stringers in an end span, none of the members that were analyzed have expended more than 50 percent of their Category D fatigue life or 25 percent of their Category C life (Table 3).

Adjustments were made in the stress range to account for local effects detected by field instrumentation, impact, and double track (see notes, Table 3). An impact factor was applied to the stringers and hangers only because it was judged that the longer tributary length of the other components reduced impact effects. The factor of 1.10 is conservative because the speed limit of the trains is 20 mph, and other researchers have obtained lower factors for higher-speed traffic. For example, Kritzler (*7*) obtained an impact factor of 1.08 at 50 mph. An adjustment for double track was necessary because the stress ranges were calculated for one train using the near track. The adjustment accounts for 47.5 percent of the trains using the near track, 47.5 percent of the trains using the far track, and 5 percent of the trains using both tracks concurrently.

Few of the stress cycles for the typical hanger exceed the Category D fatigue limit of 7 ksi; therefore, it is unlikely that these members accumulate fatigue damage. The other truss members have expended between 14 percent and 43 percent of their fatigue life in Category D or between 7 percent and 22 percent of their fatigue life in Category C. The diagonal has suffered the most fatigue damage; its remaining fatigue life is 30 years. This estimate allows for a 5 percent increase in both stress range and cycles per year. In addition, the draw movement stress range is increased to 16 ksi (after 20 percent

TABLE 3 Cumulative Fatigue Damage for Selected Members

Member	S_{re} (ksi)	n_i to 1989 ($\times 10^6$)	N_i, Category D ($\times 10^6$)	D_i, Category D	N_i, Category C ($\times 10^6$)	D_i, Category C
Framed Hanger (13–14)						
Traffic	2.3[a]	28	180	0.16	365	0.08
Draw motion	11.2[b]	0.27	1.55	0.18	3.2	0.09
Total				0.34		0.17
End Post (13–15)						
Traffic	3.5[c]	1.05	51	0.02	103	0.01
Draw motion	13.6[b]	0.27	0.88	0.32	1.78	0.16
Total				0.34		0.17
Top chord (11–13)						
Traffic	3.9[c]	0.99	36	0.03	74	0.01
Draw motion	9.7[b]	0.27	2.4	0.11	5	0.06
Total				0.14		0.07
Diagonal (8–7)						
Traffic	2.4[c]	18.4	164	0.11	334	0.06
Draw motion	13.7[b]	0.27	0.85	0.32	1.74	0.16
Total				0.43		0.22
Stringers (traffic only)						
Panels 0–2 (I = 1.2)	4.2[d]	14	30	0.47	54	0.26
Panels 2–16 (I = 1.1)	3.8[d]	14	40	0.35	80	0.18
Panels 16–18 (I = 1.2)	4.7[d]	14	22	0.64	44	0.32

[a]Hangers: local effects (1.20) × impact (1.10) × double track* (0.86) = 1.15.
[b]Draw span motion only: local effects = 1.20.
[c]Chord member traffic loads: local effects (1.20) × double track* (0.86) = 1.03.

Near track	0.475	(1)	= 0.475
Far track	0.475	(0.4)	= 0.030
Both tracks	0.05	(1.4)	= 0.137
	Result of addition		0.642
	$(0.642)^{1/3}$		= 0.866

[d]Stress range at bolt hole, flange angle to web plate connection.
*Double-track root mean cube adjustment based on Miner's rule and typical S-N curves.

adjustment for local effects) to account for planned modifications that will increase the lift angle to 75 degrees. Draw span movement contributes the most to fatigue damage for end post (Member 13-15), the top chord (Member 11-13), and the diagonal (Member 8-9), whereas draw span movement and freight traffic contribute almost equally to fatigue damage for the framed hanger (Member 13-14).

The bottom end post (Member 15-17) also has substantial stress ranges (Figure 4) but was not analyzed in detail during this study. The large stress ranges are partially due to bending moments near Node 17. The stresses are most likely altered by several large gusset plates that reinforce the end trunnion that were not modeled in the frame analysis. Further field instrumentation or a more refined analysis should be undertaken before the damage index for Member 15-17 is estimated.

The peak stresses for the typical stringers (Panels 2 through 16) is at the fatigue limit of 7 ksi. The peak stresses for stringers in the end span (Panels 16 through 18) are somewhat higher. If the stringers accumulate fatigue damage, they accumulate it faster than other members. Considering the design of the bridge and the location of the stringer, this is a reasonable conclusion. Except for the stringers, all of the members of the bridge were designed to resist the load of two trains; however, most cyclic loads are the result of one train's passage. The stringers receive more cycles because of their short tributary length even though only half of the trains use each stringer.

Impact factors of 1.10 and 1.20 were assigned to the intermediate (Panels 2–16) and end (Panels 0–2, 16–18) stringers, respectively. The higher-impact factor was selected for the end stringers because special rail joints exist near the supports and are likely to increase impact loading. This is consistent with the results of a study about the effect of rail defects on impact loading (*13*). The stress ranges for the nontypical stringers (Panels 0–2 and 16–18) were estimated by calculating an equivalent fatigue load (EFL) from the stress range and section properties of a typical stringer and applying this load to the nontypical stringers. The geometry of the EFL is similar to a rail car's wheel set (Figure 3*a*), and the wheel load is 21 kips. For Stringer Panel 16–18, the remaining Category D and C fatigue life is estimated at 7 and 25 years, respectively. The remaining Category D fatigue life of a typical (Panels 2–16) stringer is estimated at 22 years. These estimates allow for a 5 percent increase in cyclic stresses and the number of cycles per year. At the end of the Category D service life, an abrupt failure of the entire member is not expected. As stated earlier, Category D indicates the lower bound for the fatigue strength of an individual component in a built-up member (*12*). It is likely that cracks may be detected as they occur and the individual components replaced to extend the life of the member.

The service life of the stringer-to-floor-beam connection was also investigated (*10*). The calculations are sensitive to changes in assumptions regarding the joint's fixity, which was not known with certainty; however, the results show that it is possible that these connection angles have reached the end of their design fatigue life. This possibility may be determined by regular inspection. Since the connection is supported by two angles, both would have to crack before the connection would collapse. If cracks were detected, the angles could be replaced at a relatively low cost.

CONCLUSIONS AND RECOMMENDATIONS

It is concluded that most of the components in BN's Bridge 4, except for the stringers, have a remaining fatigue service life of at least 30 years. The service life of many of the components may be much longer. Of the components analyzed, it is expected that the end stringers will be the first major components to reach the end of their service life. It is likely that service life may be extended by replacing individual components of built-up members as cracks occur.

Comparisons with weigh-in-motion data and instrumentation results show that computerized train lists are a valuable source of data that may be used in the development of current load spectrums.

Two possible methods were identified that could be used to generalize site-specific fatigue information. If an estimate exists for the number of TPC for a particular type of member (perhaps a stringer of a certain length), the number of cycles per year can be estimated if the gross annual tonnage is known and the traffic mix is similar. Since railroads routinely collect data on gross annual tonnage, this information is easily available.

If a set of EFLs could be developed by calculating the wheel loads that would cause the equivalent stress range for certain members, these EFLs could be used to estimate the equivalent stress range in similar members. Ultimately, the EFLs could be developed into a fatigue train that would be similar in concept to the fatigue truck that was proposed by Moses et al. (*14*).

ACKNOWLEDGMENT

Funding for this project was provided by Burlington Northern's Research and Development Department and Trans-Now, U.S. Department of Transportation's Region 10 University Transportation Center. This support is gratefully acknowledged.

REFERENCES

1. Steel Bridges, Chapter 15. In *Manual for Railroad Engineering*, American Railway Engineering Association, 1989.
2. Z. Prucz and W. B. Conway. Extending the Fatigue Life of the US 190 Mississippi River Bridge, Baton Rouge, Louisiana. *Proc., 6th Annual International Bridge Conference*. Pittsburgh, Pa., June 1989, pp. 308–316.
3. R. A. P. Sweeney. The Load Spectrum for the Fraser River Bridge at New Westminster, B. C. *Area Bulletin 658*, 1976.
4. P. Grundy. Fatigue Life of Australian Railway Bridges. *Civil Engineering Transactions*. The Institution of Civil Engineers, Australia, 1982.
5. E. A. Ebrahimpour, E. A. Maragakis, and D. N. O'Connor. On Fatigue Evaluation of Riveted Connections in Railway Bridges. *Proc., Firth of Fourth Bridge Centenary Conference*, Edinburgh, Scotland, Aug. 1990.
6. J. W. Fisher and J. Hartley Daniels. An Investigation of the Estimated Fatigue Damage in Members of the 380-ft. Main Span, Fraser River Bridge. *AREA Bulletin*, No. 658, 1976.
7. R. W. Kritzler. Rating of Railroad Bridges by Field Load Testing. *Proc., 6th Annual International Bridge Conference*, Pittsburgh, Pa., June 1989, pp. 171–178.

8. D. A. Foutch, S. D. Schiff, and J. Choros. Development of Load Spectra for Railway Bridges Under Changing Operating Conditions. *Proc., 6th Annual International Bridge Conference*, Pittsburgh, Pa., June 1989, pp. 179–192.
9. E. L. Wilson and A. Habibullah. *SAP90 Users Manual*. Computers and Structures, Inc., Berkeley, Calif., 1989.
10. J. A. Rooker. Fatigue Life Investigation of Ballard Railway Bridge. M.S. thesis. University of Washington, Seattle, 1989.
11. C. G. Shilling. Stress Cycles for Fatigue Design of Steel Bridges. *Journal of the Structural Division*, ASCE, Vol. 110, No. 6, June 1984, pp. 1222–1234.
12. J. W. Fisher, B. T. Yen, D. Wang, and J. E. Mann. *NCHRP Report 302: Fatigue and Fracture Evaluation for Rating Riveted Bridges*. TRB, National Research Council, Washington, D.C., 1987.
13. J. F. Muller and P. F. Dux. Pre Stressed Concrete Bridge Line Load Stresses Due to Heavy Haul Coal Traffic. *Proc., Fourth International Heavy Haul Railway Conference*, Brisbane, Australia, 1989.
14. F. Moses, C. G. Schilling, and K. S. Raju. *NCHRP Report 299: Fatigue Evaluation Procedures for Steel Bridges*. TRB, National Research Council, Washington, D.C., 1987.

Publication of this paper sponsored by Committee on Steel Bridges.